

Enzyme Inhibition Assays Using Fluorescence Correlation Spectroscopy: A New Algorithm for the Derivation of $k_{\text{cat}}/K_{\text{M}}$ and K_{i} Values at Substrate Concentrations Much Lower than the Michaelis Constant

Franz-Josef Meyer-Almes*[‡] and Manfred Auer[§]

EVOTEC Analytical Systems GmbH, Max-Planck-Strasse 15a, 40699 Erkrath, Germany, and Novartis Forschungsinstitut, Brunnerstrasse 59, A-1235 Vienna, Austria

Received January 11, 2000; Revised Manuscript Received June 23, 2000

ABSTRACT: A new mathematical formalism is deduced which allows for the calculation of the k_{cat} over K_{M} ratio based on measurements of the enzyme kinetics with substrate concentrations much lower than K_{M} . The equations are also applied on the action of an inhibitor on enzyme activity yielding the binding constant, K_{i} , of an inhibitor molecule. For practical evaluation of the new theoretical approach, the enzymatic reaction of CD45 phosphatase was used as a well-characterized model system with known inhibitors for testing the K_{i} value determination scheme. The $k_{\text{cat}}/K_{\text{M}}$ ratio was calculated to be $4.7 \times 10^5 \text{ M}^{-1} \text{ s}^{-1}$, the K_{i} of the inhibitor molecule PKF52-524 was estimated to be $(1-2) \times 10^{-7} \text{ M}$ and the association rate of the inhibitor PKF52-524 to CD45 phosphatase was estimated to be $59 \text{ M}^{-1} \text{ s}^{-1}$.

The measurement of enzyme kinetics and the derivation of the Michaelis constant, K_{M} , and the turnover number, k_{cat} , is a standard approach in order to determine enzyme efficiency. Brown (1) was the first who proposed a reliable general model of enzyme action which was strictly intuitive and lacked a mathematical foundation. Then it was Henri (2) who advanced a mathematical treatment of this model but he did not derive an analytical solution of the system of differential equations. Michaelis and Menten (3) proved the validity of Henri's formalism by defined and controlled experiments. They assumed that the enzyme–substrate complex was in equilibrium with the reactands. Haldane and Briggs (4) showed that the equilibrium concept of Michaelis and Menten was not essential and demonstrated that enzyme action could be described satisfactorily using a steady-state approach. Their formalism is traditionally regarded and used as that of Michaelis and Menten. The steady-state treatment is based on the hypothesis that the concentration of the enzyme–substrate complex does not change during the course of the reaction. The temporal change of intermediate complex concentration should be small compared to the rate of substrate utilization. This point was elaborated by Wong (5).

Traditionally, the most common way to determine the Michaelis constant and turnover rate was to measure the initial rate over a small range of the reaction for which the change in substrate concentration is negligible compared to the total substrate available, which is usually much higher concentrated than the enzyme. There are several drawbacks associated with experiments using high substrate concentrations.

First, it is more probable that substrate aggregates will be formed which complicate the reaction mechanism, or even render the substrate incapable of being processed by the enzyme. This would obscure K_{M} and k_{cat} values since they would be determined without considering substrate aggregation. Second, at high substrate concentration, it becomes more likely that more than one substrate molecule binds to the enzyme. This could yield enzyme–substrate complexes which could be activated or inhibited compared to the enzyme–substrate complex with 1:1 ratio. K_{M} and k_{cat} values determined under these conditions would also be inaccurate.

Third, if the substrate of the enzymatic reaction is a large molecule like for protein kinases or protein phosphatases, substrate excess might be difficult to achieve experimentally. Forth, in new detection methods for miniaturized screening, like fluorescence correlation spectroscopy, low (nanomolar) amounts of fluorescently labeled substrate are a prerequisite to achieve single molecule detection conditions.

These arguments emphasize the requirement for evaluating enzyme reactions with low substrate concentrations, when the traditional Michaelis approach cannot be applied. Reiner and Schulz (6, 7) used complex equations which took the mass conservation of substrate concentration into account to analyze enzyme reactions. But these equations were not convenient to work with. In principle, the time course of substrate, intermediate, and product can be compared with analytical mathematical solutions of systems of differential equations for enzyme-catalyzed reactions which are described, e.g., by Kuchel (8) and Cantor and Schimmel (9) or in this study (see eq 3). This kind of analysis of enzyme kinetics requires time-resolved data of at least one or, better, two molecular entities involved in the enzyme reaction and would be an iterative troublesomely process. Forsblom et al. (10) treated the elementary steps of single substrate binding and catalytic cleavage of the substrate to the product

* To whom correspondence should be addressed.

[‡] EVOTEC Analytical Systems GmbH.

[§] Novartis Forschungsinstitut.

by the eigenvalue approach. They have been able to analyze the kinetics of DNA cleavage by restriction endonuclease *EcoRI* at very low substrate concentrations. This approach was based on the assumption of a rapid preequilibrium and not extended to enzyme inhibition.

In the present study a new formalism is deduced which allows for the calculation of the k_{cat} over K_M ratio based on measurements of the enzyme kinetics with substrate concentrations much lower than K_M . An extension of our approach allows the calculation of binding constants of enzyme inhibitors from measurements of enzyme kinetics in the presence and absence of inhibitor molecules.

For practical evaluation of the new theoretical approach the enzymatic reaction of CD45 phosphatase was used as a well characterized model system with known inhibitors for testing the K_i value determination scheme. CD45 phosphatase plays a pivotal role in antigen stimulated proliferation of T-lymphocytes. It activates two src-family protein tyrosine kinases Fyn and Lck by dephosphorylating the negative regulatory tyrosine residue (11).

MATERIALS AND METHODS

The plasmids for bacterial expression of the DID2 catalytic domains of human CD45 under control of the T7-promoter were obtained from H. Saito (Dana Farber Cancer Institute). CD45 PTPase¹ was purified from *Escherichia coli* BL21 cultures by ammonium-sulfate precipitation and three chromatographic separations on DEAE sepharose, blue sepharose, and phospho-cellulose columns, respectively (12, 13). The final enzyme preparation was >80% pure as indicated by Coomassie/silver staining after SDS-PAGE under reducing conditions. The enzyme stock solution (25 $\mu\text{g}/\text{mL}$ in 16 mM Tris-HCl, pH 8, 1.25 mM EDTA, 25 mM NaCl, 5 mM 2-mercapto-ethanol, and 50% glycerol) was stored frozen in aliquots at -80°C .

The labeled lck-peptide substrate, 5,6-TAMRA-6-Ahx-TEGQY(PO₃H₂)QPQP, containing a phosphorylated tyrosine was synthesized at Novartis according to standard peptide synthesis procedures. The peptide concentration was calculated from its dry weight. The calculated concentration agreed with the particle number of the FCS experiment with a confocal volume element of 0.5×10^{-15} L. The inhibitor PKF52-524 had been identified in an ELISA-based high throughput screen at Novartis Forschungsinstitut. Anti-phosphotyrosine antibody (PT 66) was purchased from SIGMA. Its concentration was determined using the BCA protein assay of Pierce. Simulations were done using the program MathCad (MathSoft). Enzyme kinetics were measured using Fluorescence Correlation Spectroscopy (FCS), and the experiments were carried out on a ConfoCor (Carl Zeiss, Jena/EVOTEC BioSystems AG, Hamburg) equipped with helium-neon laser (543 nm line, Uniphase), C-APOCHROMAT 40 \times /1.2 objective (Carl Zeiss Jena), interference filter 605DF50 (Omega) and a pinhole with 40 μm diameter. The photon count signals were autocorrelated over a period of 20 s.

¹ Abbreviations: TAMRA, tetramethylrhodamine; Ahx, aminohexanoic acid; ELISA, enzyme-linked immunosorbent assay; FCS, fluorescence correlation spectroscopy; SDS-PAGE, sodium dodecyl sulfate-polyacrylamide gel electrophoresis; Tris, tris-(hydroxymethyl)-aminomethane; EDTA, ethylenediaminetetraacetic acid; DEAE, diethylaminoethyl; PTPase, protein tyrosine phosphatase.

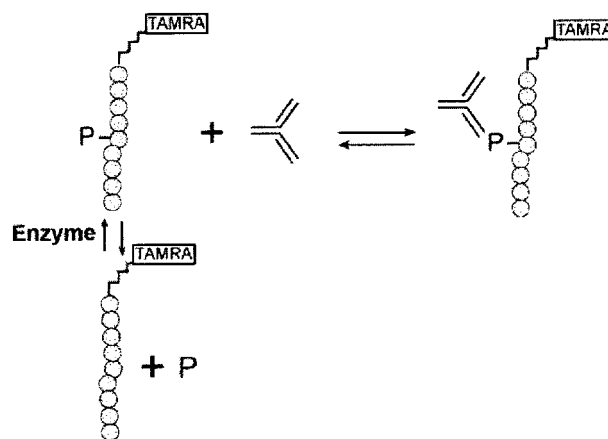


FIGURE 1: CD45 phosphatase assay scheme.

Reaction Conditions. In the majority of the enzyme activity experiments, 12.5 nM TAMRA-lck-peptide and 10 nM CD45 tyrosine phosphatase were incubated at $(22 \pm 2^\circ\text{C})$. The reaction was stopped by the addition of a mixture of 100 nM antiphosphotyrosine antibody and 30 mM H₂O₂ (Figure 1). The percentage of slow diffusing complexes consisting of antibody and unprocessed substrate peptide was measured using FCS. Mean diffusion times of unbound substrate peptide and the complex comprising peptide and antibody through the observation volume were (190 ± 8) and (570 ± 28) μs , respectively.

Data Evaluation. Evaluation of the autocorrelation curves was carried out with a Marquardt nonlinear least-squares fitting routine using the following two-component model corresponding to free and bound TAMRA-lck-peptide:

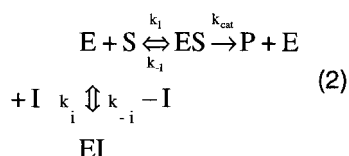
$$G(\tau) = \left[1 - T + T \exp\left(\frac{-\tau}{\tau_T}\right) \right] N^{-1} \times \left[\frac{1 - Y}{\left(1 + \frac{\tau}{\tau_{\text{free}}}\right) \sqrt{1 + \frac{r_0^2}{z_0^2} \frac{\tau}{\tau_{\text{free}}}}} + \frac{Y}{\left(1 + \frac{\tau}{\tau_{\text{bound}}}\right) \sqrt{1 + \frac{r_0^2}{z_0^2} \frac{\tau}{\tau_{\text{bound}}}}} \right] \quad (1)$$

where T is the average fraction of dye molecules in the triplet state with relaxation time τ_T , N is the total average number of fluorescent molecules in the observation volume, Y is the relative concentration fraction of bound TAMRA-lck-peptide with respect to the total peptide concentration, τ_{free} and τ_{bound} define the average diffusion times for detected free and bound peptide molecules, respectively, and r_0 and z_0 are the lateral and axial distances between the coordinate where the Gaussian emission light distribution attains the maximum value and the point where the light intensity decreases to $1/e^2$ of the maximum value (observation volume). Equation 1 is only valid, if the relaxation time τ_{chem} of the chemical reaction between free and bound TAMRA-lck-peptide is much larger than the diffusion time τ_{diff} . The K_d of the antibody antigen interaction is about 1 nM. With a diffusion-controlled association rate of $10^7 \text{ M}^{-1} \text{ s}^{-1}$ the dissociation rate is calculated to be 10^{-2} s^{-1} . Using a concentration of 100 nM of antibody and 12.5 nM TAMRA-lck-peptide, τ_{chem} can be estimated to be roughly 1 s, which is much larger than τ_{diff} of the antibody-peptide complex (570 μs). Therefore, eq 1 can be applied to all experimental data.

Simulations. The system of ordinary differential equations which describe the Michaelis–Menten model have been solved numerically using the Rosenbrock method (14) in order to calculate the temporal change in concentration of the molecular species under investigation during the course of the reaction. The differential equations of the enzyme reaction with competitive inhibition are summarized in eq 3.

RESULTS

Theory. The conventional Michaelis–Menten model with competitive inhibition (eq 2) is the basis of the following mathematical transformations which yield a simple expression for the description of enzyme reaction at substrate concentrations significantly below the K_M



where E = enzyme, S = substrate, ES = complex of E and S, P = product, I = inhibitor, EI = complex of E and I. The sequence of chemical reactions as depicted in eq 2 is described by the following system of ordinary differential equations (eq 3):

$$\begin{aligned} \frac{d[\text{E}]}{dt} &= -k_1[\text{E}][\text{S}] + (k_{-1} + k_{\text{cat}})[\text{ES}] - k_i[\text{E}][\text{I}] + k_{-i}[\text{EI}] \\ \frac{d[\text{S}]}{dt} &= -k_1[\text{E}][\text{S}] + k_{-1}[\text{ES}] \\ \frac{d[\text{ES}]}{dt} &= k_1[\text{E}][\text{S}] - (k_{-1} + k_{\text{cat}})[\text{ES}] \\ \frac{d[\text{P}]}{dt} &= k_{\text{cat}}[\text{ES}] \\ \frac{d[\text{I}]}{dt} &= -k_i[\text{E}][\text{I}] + k_{-i}[\text{EI}] \\ \frac{d[\text{EI}]}{dt} &= k_i[\text{E}][\text{I}] - k_{-i}[\text{EI}] \end{aligned} \quad (3)$$

with the initial conditions as $[\text{P}]_0 = 0$, $[\text{ES}]_0 = 0$, and $[\text{EI}]_0 = 0$ and the conservation laws as $[\text{E}] = [\text{E}]_0 - [\text{ES}] - [\text{EI}]$, $[\text{S}] = [\text{S}]_0 - [\text{ES}] - [\text{P}]$, and $[\text{I}] = [\text{I}]_0 - [\text{EI}]$.

Enzyme Reaction without Inhibitor ($[\text{I}]_0 = 0$). Under the conditions of very low substrate concentration and catalytic enzyme concentration, it is assumed that only a small fraction of the available enzyme is utilized ($[\text{ES}] \approx 0$) and that the intermediate concentration $[\text{ES}] \ll [\text{E}]_0$, $[\text{S}]_0$ during the measurement. Therefore, $[\text{E}] \approx [\text{E}]_0$. The assumption is verified by simulations of the time course of ES. (For example, if $k_1 = 10^7 \text{ M}^{-1} \text{ s}^{-1}$, $k_{-1} = 10^4 \text{ s}^{-1}$, $k_{\text{cat}} = 300 \text{ s}^{-1}$, $[\text{S}]_0 = 12.5 \text{ nM}$, and $[\text{E}]_0 = 10 \text{ nM}$, then the concentration of intermediate ES is less than 10^{-13} M after 50 s, when the first FCS measurement is carried out.)

If $[\text{E}] \approx [\text{E}]_0$, then

$$\begin{aligned} \frac{d[\text{E}]}{dt} &= -k_1[\text{E}]_0[\text{S}] + (k_{-1} + k_{\text{cat}})[\text{ES}] = 0 \\ \Leftrightarrow [\text{ES}] &= \frac{k_1}{k_{-1} + k_{\text{cat}}}[\text{E}]_0[\text{S}] \end{aligned} \quad (4)$$

Substitution into $d[\text{P}]/dt = k_{\text{cat}}$ yields

$$\frac{d[\text{P}]}{dt} = \frac{k_1 k_{\text{cat}}}{k_{-1} + k_{\text{cat}}}[\text{E}]_0[\text{S}] \quad (5)$$

Simple transformations yield

$$\frac{d[\text{S}]}{dt} = -\frac{d[\text{P}]}{dt} \quad (6)$$

The analytical solution of the differential equation $d[\text{S}]/dt = [(-k_1 k_{\text{cat}})/(k_{-1} + k_{\text{cat}})][\text{E}]_0[\text{S}]$ with respect to substrate concentration is

$$[\text{S}] = [\text{S}]_0 \exp\left(-\frac{t}{\tau}\right)$$

with

$$\tau = \frac{k_{-1} + k_{\text{cat}}}{k_1 k_{\text{cat}}[\text{E}]_0} = \frac{K_M}{k_{\text{cat}}[\text{E}]_0} \quad (7)$$

This means that the ratio of turnover number k_{cat} and the Michaelis constant K_M which characterizes the efficiency of a certain enzyme can be simply calculated from the time constant of the enzyme kinetics, if the enzyme concentration is known.

Enzyme Reaction with Inhibitor. The impact of an inhibitor on the enzymatic activity is usually measured after mixing of the inhibitor with substrate and initiating the reaction by subsequent addition of enzyme. Given a very low substrate concentration and a slow association rate, this leads to a complex time course for the molecular species involved. If the chemical equilibrium between inhibitor and enzyme is established before the reaction is started by addition of substrate, the following presuppositions and assumptions can be made in order to simplify the equations which allow for the calculation of the equilibrium constant of the inhibitor, K_i :

1. $[\text{I}]_0 \gg [\text{E}]_0$
2. $[\text{ES}] \ll [\text{E}]_0$, then $[\text{E}]_0 = [\text{E}] + [\text{EI}]$
3. $\frac{d[\text{EI}]}{dt} = \frac{d[\text{E}]}{dt} = 0$

K_i is defined to be the ratio of k_{-i}/k_i . Therefore,

$$K_i = \frac{k_{-i}}{k_i} = \frac{[\text{E}][\text{I}]_0}{[\text{EI}]} \Leftrightarrow [\text{EI}] = \frac{[\text{E}]_0[\text{I}]_0}{K_i + [\text{I}]_0} \quad (9)$$

The enzyme concentration does not change (see above):

$$\begin{aligned} -\frac{d[\text{E}]}{dt} &= -k_1[\text{E}][\text{S}] + (k_{-1} + k_{\text{cat}})[\text{ES}] - k_i[\text{E}][\text{I}] + k_{-i}[\text{EI}] = 0 \end{aligned}$$

$$\Leftrightarrow [ES] = \frac{k_1}{k_{-1} + k_{cat}}[E][S]$$

$$\Leftrightarrow [ES] = \frac{k_1}{k_{-1} + k_{cat}}[S] \left([E]_0 - \frac{[E]_0[I]_0}{K_i + [I]_0} \right) \quad (10)$$

Since $d[S]/dt = -d[P]/dt$, the following equations can be deduced:

$$\frac{d[S]}{dt} = -\frac{d[P]}{dt} = -k_{cat}[ES]$$

$$\Leftrightarrow \frac{d[S]}{dt} = \frac{-k_1 k_{cat}}{k_{-1} + k_{cat}}[S] \left([E]_0 - \frac{[E]_0[I]_0}{K_i + [I]_0} \right) \quad (11)$$

$$\Leftrightarrow \frac{d[S]}{dt} = \frac{-k_{cat}}{K_M} \left(1 - \frac{[I]_0}{K_i + [I]_0} \right) [E]_0 [S]$$

The solution of the differential equation is

$$[S] = [S]_0 \exp\left(-\frac{t}{\tau}\right) \text{ with } \tau = \frac{K_M}{k_{cat}[E]_0 \left(1 - \frac{[I]_0}{K_i + [I]_0} \right)} \quad (12)$$

The ratio of the time constants in the presence (τ_{+I}) (see eq 12) and in the absence of inhibitor (τ_{-I}) (see eq 7) is given below:

$$\frac{\tau_{-I}}{\tau_{+I}} = \frac{K_i}{K_i + [I]_0}$$

Rearrangement of the equation yields

$$[I]_0 = K_i \frac{1 - \left\langle \frac{\tau_{-I}}{\tau_{+I}} \right\rangle}{\left\langle \frac{\tau_{-I}}{\tau_{+I}} \right\rangle} \quad (13)$$

Range of Validity of the Equations. A preassumption of eq 7, which describes the enzyme kinetics, is that $[ES] \ll [E]_0$. This means that the enzyme kinetics is independent of substrate concentration. The amount of $[ES]$ increases if higher substrate concentrations are used. To determine the limitation of eq 7 with respect to substrate concentration, the enzyme kinetics were simulated using the parameters $k_1 = 10^7 \text{ M}^{-1} \text{ s}^{-1}$, $k_{-1} = 10^4 \text{ s}^{-1}$, $k_{cat} = 300 \text{ s}^{-1}$, and $[E]_0 = 10 \text{ nM}$. From the rate constants, K_M can be calculated to be 1.03 mM . The simulated time course of product concentration is fit using a monoexponential function with time constant τ . Various substrate concentrations and the corresponding time constants are summarized in Table 2. The time constant is virtually independent of substrate concentration until $[S]_0 = 0.01 K_M$. At $[S]_0 = 0.1 K_M$, the deviation from eq 7 is 5.8%, which could be of sufficient precision for most applications. But at $[S]_0 = K_M$, the deviation between simulated time course and eq 7 is 57%, which reflects the influence of the substrate concentration. If even higher substrate concentrations, e.g., $10 K_M$, are used the exponential increase of product concentration becomes linear and eq 7 is no longer able to describe the data.

Table 1: K_i -Values Calculated for Measurements with Different Concentrations of PKF52-524 According to Eq 13

inhibitor concentration $[I]_0$ (μM)	K_i (10^{-7} M)
1	15 !
2	5.8 !
3	2.1
3.5	1.9
4	1.0

Table 2: Deviation of Fit Enzyme Reaction Time Constant τ from Eq 7^a

$[S]_0$ (M)	τ (s)	deviation (%)
10^{-8}	343	0
10^{-7}	343	0
10^{-6}	343	0
10^{-5}	345	0.6
10^{-4}	363	5.8
10^{-3}	538	57
10^{-2}	<i>b</i>	<i>b</i>

^a Deviation of fit enzyme reaction time constant τ from eq 7 with respect to substrate concentration $[S]_0$. $K_M = 1.03 \text{ mM}$, $[E]_0 = 10 \text{ nM}$, $k_{cat} = 300 \text{ s}^{-1}$. ^b Product formation is no longer described by a single exponential

A plot of $[I]_0$ versus $[1 - \langle \tau_{-I}/\tau_{+I} \rangle] / \langle \tau_{-I}/\tau_{+I} \rangle$ is linear with a slope of K_i and an intercept of 0 (eq 13). The theory has been tested by simulations of the kinetics of the enzymatic reaction at several inhibitor concentrations.

Equation 13 describes the impact of competitive inhibitors on the activity of an enzyme when the substrate concentration and enzyme concentration are much smaller than K_M and if $K_i \gg [E]_0$.

In fact, the agreement between simulated and fitted K_i values (K_i is identical with the slope of a plot of $[I]_0$ versus $[1 - \langle \tau_{-I}/\tau_{+I} \rangle] / \langle \tau_{-I}/\tau_{+I} \rangle$) is perfect when $[E]_0 = 10 \text{ nM}$ and $K_i = 1 \mu\text{M}$ (Figure 2A). If $K_i = [E]_0 = 10 \text{ nM}$, the data begin to deviate from the theoretical linear behavior, but the deviation between input K_i and fit K_i remains small (theoretical, 10 nM ; calculated, 10.9 nM ; Figure 2B). If K_i is chosen to be $1/10$ of $[E]_0$ ($K_i = 1 \text{ nM}$ and $[E]_0 = 10 \text{ nM}$), a plot of the simulated data curves downward in a concave manner and clearly deviates from linear form. The K_i obtained when fitting a selected range of data is significantly different from the input value used for the simulation procedure (Figure 2C).

In summary, deviation from the linear behavior of a plot of $[I]_0$ versus $[1 - \langle \tau_{-I}/\tau_{+I} \rangle] / \langle \tau_{-I}/\tau_{+I} \rangle$ indicates a K_i lower than the starting concentration of the enzyme $[E]_0$. All K_i values higher or equal than $[E]_0$ can be calculated from the slope of the plot with less than 10% deviation from the theoretical K_i value.

EXPERIMENTS:

Enzyme Kinetics of CD45 Phosphatase. The dephosphorylation kinetics of the TAMRA-labeled lck-peptide substrate by CD45 phosphatase was measured by mixing substrate and enzyme and by stopping the reaction after different points in time by adding a mixture of 100 nM antiphosphotyrosine antibody and $30 \text{ mM H}_2\text{O}_2$. The CD45 phosphatase was completely inactivated within less than 1 min, whereas the binding of anti-phosphotyrosine antibody to phosphorylated peptide substrate was not disturbed. The dephosphorylation

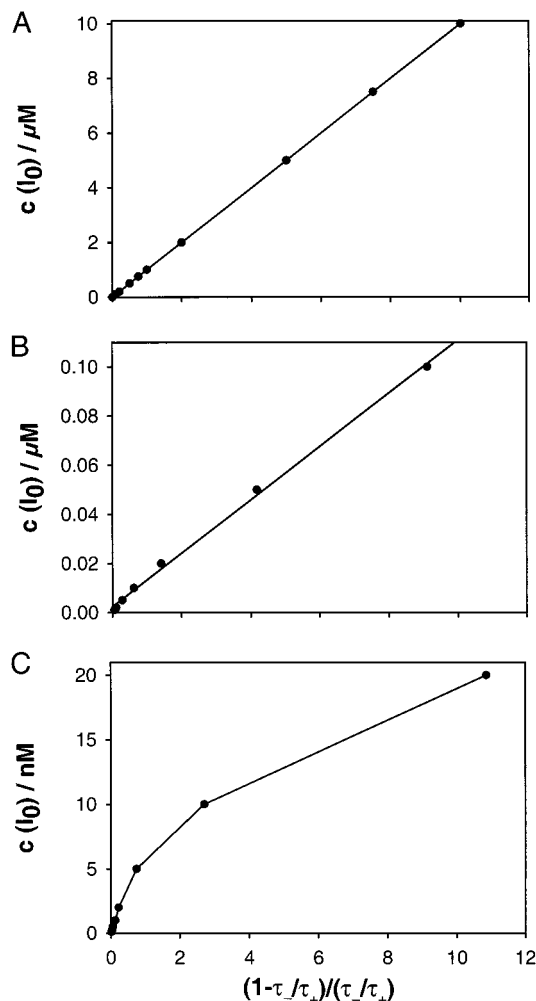


FIGURE 2: Starting concentrations of inhibitor are plotted versus $(1 - \tau_-/\tau_+)/(\tau_-/\tau_+)$. Where τ_- and τ_+ denote the time constants of simulated substrate turnover in absence and presence of inhibitor. Simulated data of enzyme kinetics are (A) $K_i = 1 \mu\text{M}$, (B) $K_i = 10 \text{ nM}$, (C) $K_i = 1 \text{ nM}$. The off rates (A) $k_{-i} = 10^{-3} \text{ s}^{-1}$, (B) 10^{-5} s^{-1} , (C) 10^{-6} s^{-1} of the inhibitor enzyme complex were used. The following parameters were used in simulations A–C: $[E]_0 = 10 \text{ nM}$, $[S]_0 = 12.5 \text{ nM}$, $k_1 = 10^7 \text{ M}^{-1} \text{ s}^{-1}$, $k_{-1} = 10^4 \text{ s}^{-1}$, $k_{\text{cat}} = 300 \text{ s}^{-1}$, $k_i = 1000 \text{ M}^{-1} \text{ s}^{-1}$. The data points in panels A and B were fit by linear regression.

kinetics fits well to a monoexponential decay with a time constant of 214 s at $[E]_0 = 10 \text{ nM}$. Therefore, the k_{cat}/K_M ratio is estimated to be $4.7 \times 10^5 \text{ M}^{-1} \text{ s}^{-1}$ using eq 7.

Association Kinetics of PKF52-524 and CD45 Phosphatase. After incubating a mixture consisting of 10 nM LCA and different concentrations of inhibitor for various lengths of time, 12.5 nM TAMRA labeled lck-peptide substrate was added. The enzyme reaction was stopped after 20 min by adding a mixture of 100 nM anti-phosphotyrosine antibody and 30 mM H_2O_2 . The degree of binding was measured using FCS (see Figure 3). The inhibitor PKF52-524 and CD45 phosphatase associate with an unusually low association rate. Even at relatively high inhibitor concentrations, e.g., $7.5 \mu\text{M}$, the time constant for the kinetics was 46 min, which means that the dephosphorylation kinetics (time constant for substrate turnover with $[E]_0 = 10 \text{ nM}$ and $[S]_0 = 12.5 \text{ nM}$ is about 3.6 min) is much faster than the association of the inhibitor. This explains the fact that in initial experiments no significant inhibition could be observed when TAMRA-lck peptide and PKF52-524 were premixed and both inhibitor

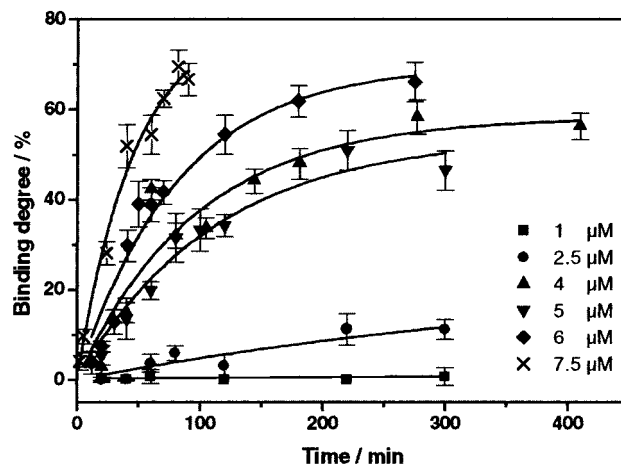


FIGURE 3: Binding degree of TAMRA-lck peptide to the anti-phosphotyrosine antibody is plotted versus time. The association kinetics of 10 nM CD45 phosphatase and different concentrations of inhibitor PKF52-524 has been measured by incubating the enzyme and the inhibitor for the noted periods of time and performing a subsequent enzyme reaction on the TAMRA-lck peptide for 20 min at $(22 \pm 2)^\circ\text{C}$.

association and dephosphorylation were started at the same time by addition of CD45 phosphatase.

To estimate the association rate, the inverse time constants of the association curves were plotted against the starting concentration $[I]_0$ of PKF52-524. Since $[I]_0$ was much higher than $[E]_0$, pseudo-first-order conditions were fulfilled and the slope of this plot should be the association rate according to the following equation:

$$\frac{1}{\tau} = k_{\text{ass}}[I]_0 + k_{\text{diss}} \quad (14)$$

The deduced association rate k_{ass} is $59 \text{ M}^{-1} \text{ s}^{-1}$. The dissociation rate k_{diss} cannot be determined with sufficient precision because the value appears to be close to zero and the inaccuracy in the estimation of the intercept is relatively large. A small k_{diss} is consistent with the low k_{ass} and a small K_i . This association rate is very small compared to a diffusion controlled k_{ass} of about $10^7 \text{ M}^{-1} \text{ s}^{-1}$.

The point in time when chemical equilibrium between inhibitor and CD45 phosphatase is reached, which is the presupposition for the formalism developed in eq 13, can be deduced easily. If prolonged incubation times between inhibitor and enzyme do not cause a further change in enzyme kinetics, chemical equilibrium conditions are achieved.

Estimation of the K_i Value of the Inhibitor PKF52-524. Equation 13, which describes the kinetic behavior of enzymes in the presence of very low substrate concentration, was applied to the CD45 assay. To fulfill the required preassumptions for the theoretical treatment, CD45 phosphatase and different PKF52-524 concentrations were incubated long enough to achieve chemical equilibrium. In our experiments, dephosphorylation was initiated by the addition of TAMRA-lck-peptide substrate after 14 h incubation time. The reaction was stopped at different time intervals by addition of an antibody/ H_2O_2 mixture, and FCS measurements were taken. The time courses of enzyme reactions in absence and presence of various concentrations of PKF52-524 are shown in Figure 4. The corresponding time constants were used to calculate the K_i for different inhibitor concentrations (Table

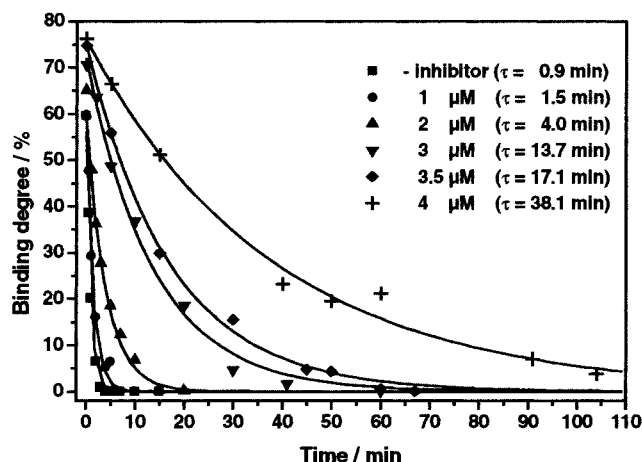


FIGURE 4: Binding degree of TAMRA-lck peptide to the anti-phosphotyrosine antibody is plotted versus time. The data depict time courses of the dephosphorylation kinetics of 12.5 nM TAMRA-lck peptide substrate using 10 nM CD45 phosphatase in absence and presence of various concentrations of the inhibitor PKF52-524 at $(22 \pm 2)^\circ\text{C}$.

1). The K_i s, calculated for each inhibitor concentration range between 1×10^{-7} and 2×10^{-7} M with exception of those for the two lowest concentrations, which are significantly higher. Maybe one reason for this observation is that the chemical equilibrium between CD45 phosphatase and PKF52-524 was not reached, resulting in excessively rapid dephosphorylation kinetics. Another more plausible reason for the downward concave curvature could be that PKF52-524 adsorbs or decays at lower concentrations which leads to a higher free enzyme concentration and thus faster dephosphorylation kinetics. This hypothesis is supported by the fact that PKF52-524 which is stored several hours in a microcentrifuge tube loses its inhibitory activity. If the data for 1 and 2 μM PKF52-524 are neglected because of suspected enhanced surface adsorption or chemical destruction, the K_i s at the higher inhibitor concentrations, which are quite consistent, should give an estimate for K_i .

DISCUSSION

The kinetic properties of enzymes are conventionally analyzed in the steady-state according to the Michaelis–Menten model. The concentration of substrate is in excess over the enzyme concentration allowing for simplification of the mathematical description. This enables the simple evaluation of characteristic parameters such as the turnover number and the Michaelis constant, K_m , allowing to compare the activities of different enzymes. The impact of inhibitors on enzymatic activity can easily be deduced from the altered kinetics on varying inhibitor concentration (15, 16).

K_M and k_{cat} values determined under high substrate concentration conditions could be disturbed due to the possible formation of substrate aggregates or deviation from 1:1 enzyme substrate complex ratio. These problems are treated in detail by Teasdale et al. (17). It is emphasized that for systems in which the possibility of substrate aggregation has not been dismissed on other valid grounds, and particularly where kinetic data are characterized as negatively cooperative, substrate aggregation should certainly be considered. Self-association is known to occur widely with large or small molecules. Deviations of enzyme behavior

from Michaelis–Menten kinetics upon substrate aggregation are revealed in experimental examples at high substrate concentrations. Characteristic examples comprise the strong impact of cholesterol aggregation on its oxidation by cholesterol oxidase (18) and apparent substrate inhibition of the enzymes esterase E-II (19), β -galactosidase (20), and rat tissue kallikrein (21). Also the low solubility of *p*-nitroaniline which can be generated, e.g., by chymotrypsin hydrolysis of *p*-nitroanilide (22) could cause problems at high substrate concentrations.

In addition, low substrate concentrations are a prerequisite to apply single molecule analysis techniques such as FCS, since this confocal method works effectively only at sufficient low concentrations of fluorescently labeled substrate. These arguments emphasize the requirement for evaluating enzyme reactions with low substrate concentrations, when the conventional Michaelis approach cannot be applied. At sufficiently low substrate level, the substrate concentration decreases significantly in the early phase of the reaction. Simultaneously, the intermediate concentration rises rapidly within milliseconds and decays again after reaching a maximum with a rate which is similar to that of product formation. Often there is only a short time period (a few seconds or less) during which the change in intermediate concentration is approximately zero ($d[\text{ES}]/dt \approx 0$). Therefore, steady-state conditions are in many cases only met within a short time window, which is not known before the enzymatic parameters have been determined. There are difficulties in the determination of true initial rates. It is necessary to check that the change in substrate–enzyme complex concentration during the period of initial rate measurement is sufficiently small so that the observed rate is correct for each specified value of substrate concentration. After a preliminary estimate for K_M and V_{max} , one can readily calculate whether these parameters would cause a significant deviation from steady-state conditions. An expendable instrumentation (e.g., stopped flow) would be required in order to ensure very fast and efficient mixing and to enable measurements of the product formation within the time range, for which steady-state conditions are given. Several attempts for the treatment of enzyme kinetics at low substrate concentrations have been made: Substitution of a substrate conservation expression into the Michaelis equation for the concentration of the intermediate $[\text{ES}]$ yields a rather complex polynomial which is an appropriate expression for the rate of the reaction when the assumption $[\text{S}]_0 \gg [\text{E}]_0$ is not satisfied:

$$\nu = \frac{k_{\text{cat}}}{2} [(K_m + [\text{S}] + [\text{E}]) - \sqrt{(K_m + [\text{S}] + [\text{E}])^2 - 4[\text{E}][\text{S}]}] \quad (15)$$

This extended Michaelis equation (6, 7) is not convenient to work with. When substrate and enzyme levels in non-steady-state conditions are used, the rate equations can become so complex that special and tedious numerical procedures must be followed to obtain solutions. Another realistic mathematical model for low substrate concentrations was derived by Forsblom et al. (10), which helped to understand the dynamic processes involved in the cleavage of DNA from Adenovirus Type 1, Type 5, and Type 6 by

the restriction endonuclease *EcoRI*. Under the assumptions of constant enzyme concentration and a rapid preequilibrium between enzyme, substrate and their intermediate complex an eigenvalue approach revealed an expression for the experimental cleavage rate [$k = ([E]k_{\text{cat}})/([E] + K_M)$] which is similar to eq 7. Forsblom's equation was used for example to analyze the exonuclease activity of T7-DNA polymerase by Földes-Papp et al. (23).

Within this study a new simple mathematical expression is deduced which enables the calculation of k_{cat}/K_M from the transient kinetics of substrate turnover at substrate concentrations much below K_M where the intermediate concentration $[ES]$ is much smaller than the substrate and enzyme concentration. In contrast to the eigenvalue approach of Forsblom there was no assumption of a rapid preequilibrium necessary for the derivation of eq 7. Equation 7 is valid even if the relaxation time of the preequilibrium is assumed to be larger than $1/k_{\text{cat}}$, e.g., for very small k_{-1} . The mathematical treatment was also extended to enzyme inhibition and to an expression for the accurate determination of K_i .

This formalism can be applied to all enzyme reactions for which the turnover of small substrate concentrations is to be determined. The new algorithm is particularly useful for assays based on FCS or EVOTEC's proprietary FIDA read out technology (24). Because of very high sensitivity and selectivity, FCS and FIDA allow enzymatic assays to be performed at extremely low substrate concentrations. For validation of the newly deduced equations the enzyme kinetics of CD45 tyrosine phosphatase was investigated. The experimental conditions used for the CD45 phosphatase assay do not allow a large excess of substrate over enzyme because a specific N-terminally fluorescently labeled substrate peptide with a special recognition site for an anti-phosphotyrosine antibody is to be used. However, the direct antibody sensor binding site is neither chromogen nor fluorogen. Therefore, a turnover of a very tiny fraction of substrate in the presence of a high excess of unprocessed substrate is very difficult to observe. Hence, the CD45 phosphatase reaction cannot be treated according to the general steady-state Michaelis–Menten approach mentioned above in order to get the ratio k_{cat}/K_M .

The substrate turnover at $[S]_0 = 12.5$ nM and $[E]_0 = 10$ nM fits well to a monoexponential decay function. From the time constant of 214 s, a k_{cat}/K_M ratio of $4.7 \times 10^5 \text{ M}^{-1} \text{ s}^{-1}$ is calculated. This value is in reasonable agreement with $7.6 \times 10^5 \text{ M}^{-1} \text{ s}^{-1}$ which was reported by Cho et al. (25). The remaining difference could be due to slightly different temperatures or buffers. The K_i of the inhibitor molecule PKF52-524 was estimated to be $(1-2) \times 10^{-7} \text{ M}$. The association rate of the inhibitor PKF52-524 to CD45 tyrosine phosphatase was $59 \text{ M}^{-1} \text{ s}^{-1}$, which is significantly lower than for a diffusion controlled reaction. Therefore, the binding of the inhibitor to the phosphatase is assumed to be a complex reaction consisting of at least two steps. As is observed in many inhibitor-enzyme binding studies, the rate-limiting step could be a conformational change of the enzyme in order to fold the binding site of the inhibitor for optimal affinity, which is also called "induced fit". If an inhibitor would bind in a diffusion controlled manner, it could be concluded that no conformational change must take place for high affinity. Such kinetic measurements of the molecular dynamics are a valuable complement for rational drug design

based on X-ray or NMR-structure data and molecular modeling (26).

CONCLUSION

A mathematical formalism that can be applied to enzyme reactions with substrate concentrations much smaller than the Michaelis constant K_M has been developed and experimentally tested. Experimental data of CD45 phosphatase enzyme activity could be well explained by the theoretical expressions deduced. Using our novel algorithm the enzyme reaction was characterized in terms of k_{cat} over K_M ratio ($4.7 \times 10^5 \text{ M}^{-1} \text{ s}^{-1}$) as well as association rate ($59 \text{ M}^{-1} \text{ s}^{-1}$) and inhibition constant K_i [$(1-2) \times 10^{-7} \text{ M}$] of the test compound PKF52-524. Our approach opens new quantitative access to enzyme reactions and their inhibition using natural substrates which do not generate a chromogenic or fluorogenic signal change. Since FCS allows for very short measurement times of less than 2 s with high precision, the method for determining K_i values of potential inhibitor molecules provides for a new quality in high-throughput compound screening in enzymatic assays.

ACKNOWLEDGMENT

We thank Franz Hammerschmid (NFI) for the purification of CD45 PTPase, Roland Reuschel (NFI) for the synthesis of the TMR-labeled peptide, Kurt Stoeckli for numerous encouraging discussions, and Jan E. DeVries for continuous support.

ACKNOWLEDGMENT

We gratefully acknowledge the excellent technical assistance provided by Klaudia Wyzgol (EVOTEC) who performed the FCS measurements and Christine Graf (NFI).

REFERENCES

1. Brown, A. J. (1902) *J. Chem. Soc.* 81, 373.
2. Henri, V. (1903) *Lois generales de l'action des diastases*, Hermann, Paris.
3. Michaelis, L., and Menten, M. L. (1913) *Biochem. Z.* 49, 333–369.
4. Briggs, G. E., and Haldane, J. B. S. (1925) *Biochem. J.* 19, 338–339.
5. Wong, J. T.-F. (1975) *Kinetics of enzyme Mechanisms*, Academic Press, London.
6. Reiner, J. M. (1959) *Behavior of enzyme systems*, Burgess Publ. Co., Minneapolis.
7. Schulz, A. R. (1994) *Enzyme Kinetics*, Cambridge University Press, New York.
8. Kuchel, P. W. (1985) in *Organized multienzyme systems: Catalytic Properties* (Welch, G. R., Ed.) pp 303–380, Academic Press, San Diego.
9. Cantor, C. R., and Schimmel, P. R. (1980) *Biophysical Chemistry*, pp 887–978, Freeman and Company, New York.
10. Forsblom, S., Rigler, R., Ehrenberg, M., Pettersson, U., and Philipson, L. (1976) *Nucleic Acids Res.* 3, 3255–3269.
11. Trowbridge, I. S., and Thomas, M. L. (1994) *Annu. Rev. Immunol.* 12, 85–116.
12. Itoh, M., Streuli, M., Krueger, N. X., and Saito, H. (1992) *J. Biol. Chem.* 267, 12356–12363.
13. Hammerschmid, F., personal communication.
14. Wanner, G. (1987) in *Numerical Analysis, Pitman Research Notes in Mathematics* (Griffith, D. F., and Watson, G. A., Eds.) Vol. 170, Harlow, Essex, U.K.
15. Stryer, L. (1988) *Biochemistry*, Freeman and Company, New York.
16. Lehninger, A. L. (1975) *Biochemistry*, Worth Publishers, Inc., New York.

17. Teasdale, R. S., Carr, A. R., and Read, R. S. (1985) *J. Theor. Biol.* 114, 375–382.
18. Aleksandrovskii, I. A., and Titov, V. N. (1993) *Biokhimiia* 58, 1408–1419.
19. Cloeter, F., Viljoen, C. C., and Schabort, J. C. (1983) *Toxicon* 21, 857–869.
20. Pulvin, S., Friboulet, A., and Thomas, D. (1990) *Biochim. Biophys. Acta* 1041, 97–100.
21. Sousa, M. O., Rodrigues, C. V., Pena, H. B., Alvarenga, M. G., Machado-Coelho, G. L. L., Santoro, M. M., Juliano, M. A., Juliano, L., and Figueiredo, A. F. S. (1996) *Braz. J. Med. Biol. Res.* 29, 327–334.
22. Fischer, G., Ban, H., Berger, E., and Schellenberger, A. (1984) *Biochim. Biophys. Acta* 791, 87–97.
23. Földes-Papp, Z., Thyberg, P., Björling, S., Holmgren, A., and Rigler, R. (1997) *Nucleosides Nucleotides* 16, 781–787.
24. Kask, P., Palo, K., Ullmann, D., and Gall, K. (1999) *Proc. Natl. Acad. Sci. U.S.A.* 96, 13756–13761.
25. Cho, H., Krishnaraj, R., Itoh, M., Kitas, E., Bannworth, W., Saito, H., and Walsh, C. T. (1993) *Protein Sci.* 2, 977–984.
26. Davis, A. M., and Teague, S. J. (1999) *Angewandte Chemie* 111, 778–792.

BI000057Y